Titre: Photodegradation of micropollutants by vacuum-UV (VUV) radiation in potable reuse waters: Promotive and inhibitory effects of free chlorine oxidant
Title:

Auteurs: Mahsa Masjoudi, Fuhar Dixit, Benoit Barbeau, William A. Mitch, & Madjid Mohseni
Authors:

Date: 2025

Type: Article de revue / Article

Référence: Masjoudi, M., Dixit, F., Barbeau, B., Mitch, W. A., & Mohseni, M. (2025). Photodegradation of micropollutants by vacuum-UV (VUV) radiation in potable reuse waters: Promotive and inhibitory effects of free chlorine oxidant. Journal of Environmental Chemical Engineering, 13(1), 115095 (10 pages). https://doi.org/10.1016/j.jece.2024.115095
Citation:

Titre de la revue: Journal of Environmental Chemical Engineering (vol. 13, no. 1)
Journal Title:

Maison d'édition: Elsevier
Publisher:

URL officiel: https://doi.org/10.1016/j.jece.2024.115095
Official URL:

Journal of Environmental Chemical Engineering 13 (2025) 115095

Contents lists available at ScienceDirect

Journal of Environmental Chemical Engineering

journal homepage: www.elsevier.com/locate/jece

Photodegradation of micropollutants by vacuum-UV (VUV) radiation in potable reuse waters: Promotive and inhibitory effects of free chlorine oxidant

Mahsa Masjoudi [a], Fuhar Dixit [a,b], Benoit Barbeau [c], William Mitch [d], Madjid Mohseni [c,*]

[a] Department of Chemical and Biological Engineering, University of British Columbia, 2360 E Mall, Vancouver, BC, Canada
[b] Department of Civil and Environmental Engineering, University of California, Berkeley, CA, USA
[c] Department of Civil, Geological and Mining Engineering, Polytechnique Montreal, QC, Canada
[d] Department of Civil and Environmental Engineering, Stanford University, CA, USA

ARTICLE INFO

Keywords:
UV-185 nm
Emerging contaminants
Water treatment
Advanced oxidation process
Free chlorine

ABSTRACT

The occurrence of a variety of harmful micropollutants in potable reuse trains has been a matter of concern. In this study, the performance of the vacuum-ultraviolet / ultraviolet advanced oxidation process (VUV/UV AOP) without and with free chlorine (VUV/UV/Cl_2 AOP) for elimination of carbamazepine (CBZ) and 1,4-dioxane (1,4-D) from potable reuse systems was evaluated. The addition of free chlorine improved CBZ degradation by ~12 % while reducing the rate of 1,4-D removal by ~50 %, highlighting the selective effectiveness of the VUV/UV/Cl_2 AOP based on micropollutant type. The effects of operational conditions, including free chlorine dosage, solution pH and contributions of different radical species, were also determined. Both high chlorine concentrations as well as alkaline pH were shown to slow down the removal of both contaminants in the VUV/UV/Cl_2. Also, the VUV/UV/Cl_2 AOP was considered to be promising for treatment of 1,4-D in reverse osmosis (RO) permeate due to photochemical chain reactions between the added chlorine and water constituents which lead to effective formation of $Cl_2^{\bullet-}$. The findings of this research demonstrate the broader potential of the VUV/UV/Cl_2 AOP as a tailored, adaptable solution for optimizing micropollutant removal in potable reuse systems, based on contaminant type and water matrix.

1. Introduction

Population growth combined with the progression of climate change is resulting in several regions around the world experiencing water shortages and frequent long-lasting droughts [44]. As a resilient response to this crisis, water reuse has come to the forefront for producing safe and high-quality potable water from wastewater [48]. The potential occurrence of organic micropollutants in the effluents of potable reuse treatment plants is a significant concern given their potential to exert toxicity [11,16,22,25,40,42]. In order to achieve a high level of performance to eliminate organic micropollutants, potable reuse treatment trains apply a multi-barrier approach to prevent passage of contaminants into the effluent water [30]. Potable reuse trains employ reverse osmosis (RO) as a broad-screen physical removal barrier in coastal areas, where discharge of the associated concentrate to seawater is possible. In inland areas, reuse trains frequently combine ozone and biological activated carbon (O_3/BAC) as broad-screen chemical and biological barriers to the passage of contaminants. For both types of trains, advanced oxidation processes (AOPs) can be used to degrade micropollutants as a final broad-screen chemical barrier [30].

AOPs used in potable reuse trains typically degrade micropollutants by direct photolysis using 254 nm UV light and by reactions with radicals, particularly hydroxyl radicals ($^{\bullet}OH$), generated by UV light photolyzing hydrogen peroxide (H_2O_2), free chlorine ($HOCl/OCl^-$) or other oxidants [20]. However, current applications of these AOPs face several challenges, such as the high energy consumption and high concentration of chemical oxidant required for effective photolysis in UV/H_2O_2 as well as the elevated risk of disinfection byproduct (DBP) formation in UV/Cl_2 processes [27,35]. Among the many different available AOPs, vacuum-ultraviolet (VUV) – covering irradiation in the spectral range of 100 – 200 nm – has been proposed as a promising treatment for degradation of a wide range of contaminants in the water

* Corresponding author.
E-mail address: madjid.mohseni@ubc.ca (M. Mohseni).

https://doi.org/10.1016/j.jece.2024.115095
Received 4 September 2024; Received in revised form 18 November 2024; Accepted 11 December 2024
Available online 12 December 2024

matrix [46]. Conventional low pressure mercury lamps are commercially available as a source of VUV/UV irradiation consisting of two major emission lines at 185 nm and 254 nm. Under such conditions, water molecules are the main absorber of the 185 nm photons producing radicals by direct photolysis (Eqs. 1 and 2) [15]. Thus, the VUV/UV AOP has been recognized for its potential to produce $^{\bullet}OH$ by photolysis of water molecules without addition of oxidants [47].

$$H_2O \xrightarrow{h\nu_{185nm}} HO^{\bullet} + H^{\bullet} \qquad \Phi_{185nm} = 0.33 \tag{1}$$

$$H_2O \xrightarrow{h\nu_{185nm}} HO^{\bullet} + H^{+} + e^{-}_{aq} \qquad \Phi_{185nm} = 0.045 \tag{2}$$

Recently, combining the VUV/UV AOP with free chlorine has been studied as a way for improving degradation of a number of micropollutants [25,28,50,51]. Free chlorine is a commonly used oxidant in water treatment which can be effectively photolyzed at 254 nm to produce $^{\bullet}OH$ and a variety of reactive chlorine species (RCSs), including chlorine radical ($Cl^{\bullet}$). Furthermore, it has been reported that free chlorine species, HOCl and OCl^-, can also absorb 185 nm photons and undergo direct photolysis under VUV radiation (Eqs. 3 and 4) [8,10,32]. Thus, the enhanced removal of certain micropollutants observed when using the VUV/UV/Cl_2 AOP in previous research has been attributed to the synergistic effects between direct photolysis at 185 and 254 nm and the reactions involving RCSs produced by both wavelengths [53]. However, addition of oxidants to the VUV/UV AOP does not always lead to synergies; in fact, in some cases, chemical oxidants have inhibited the degradation of contaminants in the VUV/UV AOP [26]. Therefore, further investigation of the VUV/UV/Cl_2 AOP and the synergistic and/or inhibitory effects of free chlorine oxidant on the treatment performance is warranted.

$$HOCl \xrightarrow{h\nu} HO^{\bullet} + Cl^{\bullet} \qquad \begin{matrix} \Phi_{(254nm)} = 0.62 \\ \Phi_{(185nm)} = 0.7 \end{matrix} \tag{3}$$

$$OCl^- \xrightarrow{h\nu} Cl^{\bullet} + O^{\bullet} \qquad \begin{matrix} \Phi_{(254nm)} = 0.55 \\ \Phi_{(185nm)} = 0.10 \end{matrix} \tag{4}$$

In this study, carbamazepine (CBZ) – an antiepileptic medicine – and 1,4-dioxane (1,4-D) – a widely used industrial solvent – were selected as two model micropollutants of concern in water treatment and potable reuse trains and their degradation was investigated under different UV and VUV/UV AOP conditions. Given the potential toxicities of these micropollutants, different environmental agencies have recommended monitoring their levels in drinking water and developed guidance values of 40 and 50 μg L^{-1} for CBZ and 1,4-D, respectively [36,49]. Here, the degradation kinetics of the two micropollutants in the VUV/UV/Cl_2 AOP were measured and the effects of major operational conditions, including free chlorine dose and solution pH, were determined. Contributions of different radical species to micropollutant degradation in the VUV/UV/Cl_2 AOP were also estimated through competition kinetic studies under experimental conditions. Finally, the performance of the VUV/UV and VUV/UV/Cl_2 AOPs for elimination of 1,4-D was evaluated in actual water samples from potable reuse systems to capture the potential impacts of matrix constituents. The findings of this research are expected to provide useful information regarding the operational criteria of the VUV/UV/Cl_2 AOP based on the type of micropollutant and water matrix for the purpose of water treatment and potable reuse.

2. Materials and methods

2.1. Chemicals and reagents

Free chlorine was prepared freshly from a stock sodium hypochlorite solution (NaOCl) (13 % w/v, Fisher Scientific, Canada). 1,4-Dioxane (1,4-D) (+99 % ACS reagent), carbamazepine (CBZ), nitrobenzene (NB) (+99 % ACS reagent), *tert*-butanol (t-BuOH) (+99 % ACS reagent), methanol (MeOH) (HPLC plus, ≥99.9 %), and dichloromethane (DCM) (HPLC plus, ≥99.9 %) were purchased from Sigma-Aldrich, Canada. Experiments were carried out in ultrapure water (resistivity 18.2 MΩ cm) from an Elga Pure water Option-Q system (Elga Labwater, UK).

O_3/BAC effluent was obtained from a pilot potable reuse plant at the Colorado School of Mines (Golden, CO, USA). Reverse osmosis (RO) permeate was collected from an indirect potable reuse facility in California. The characteristics of the recycled wastewaters are summarized in Table 1. Water samples were filtered using 0.45 μm pre-rinsed membrane filters (Millex-HV Syringe Filters, Catalog number: SLHV033RS, Duluth, GA, USA) and stored in the dark at 4°C prior to experimentation. For VUV experiments, ultrapure nitrogen (Praxair, Canada) was purged inside the VUV lamp housing to prevent absorption of 185 nm photons by oxygen and consequent ozone formation. Details of other materials used in the studies are provided in the Supplementary Information (Section S1).

2.2. Experimental procedures

Both UV and VUV experiments were conducted in a bench-scale collimated beam reactor (Figure S1). The 254 nm collimated beam used for UV experiments contained a low-pressure (LP) mercury amalgam lamp (HVA357T5L, LightSources Inc., Orange CT USA) which prevented the emission of 185 nm radiation (Section S1). For the VUV collimated beam experiments, two identical 10 W lamps with undoped quartz envelopes, transparent to both 254 and 185 nm wavelengths, were used (Sterilight S212ROL Lamp, HomePlus Products Inc., Canada). In all VUV experiments, ultrapure nitrogen was purged into the sealed collimated beam chamber to prevent absorption of 185 nm photons by oxygen, which reduces the flux of 185 nm photons to water and results in unwanted formation of ozone. The reaction vessel in all experiments was an enclosed cylinder fashioned from Spectrosil Quartz (Starna Cells Inc., USA) that is transparent to 185 and 254 nm photons and was placed at the bottom of the collimation tube within 2 cm. A custom-made copper cuvette holder was used to allow fast heat transfer and eliminate the change of sample temperature during radiation. Samples were mixed by a magnetic stirrer during UV and VUV radiation.

UV fluence rate at 254 nm was measured (~0.61 mW cm^{-2}) using iodide/iodate actinometry and corrected with water factor and divergence factor following the standard protocol described by Bolton and Linden [3] (Section S2). In the case of VUV experiments, the VUV incident fluence rate at 185 nm, $I_{0,185nm}$, was determined experimentally by measuring $^{\bullet}OH$ production via Eq. (1) using the following procedure in which carbamazepine is a probe compound and methanol is used to

Table 1
Water quality parameters for the potable reuse water samples taken from O_3/BAC effluent and RO permeate.

Water Quality Parameter	O_3/BAC Effluent	RO Permeate
pH	7.55	6.00
UV Absorbance at 254 nm (cm^{-1})	0.134	0.006
Alkalinity (mg L^{-1} $CaCO_3$)	77	13
Carbon Content (mg C L^{-1})		
DOC	9.75	0.42
Chlorine Content (mg L^{-1} Cl_2)		
Free Chlorine	ND*	ND*
Total Chlorine	ND*	1.24
Monochloramine (NH_2Cl)	ND*	0.40
Dichloramine ($NHCl_2$)	ND*	0.84
Ion Content (mg L^{-1})		
Fluoride (F^-)	ND*	0.03
Chloride (Cl^-)	81.8	3.85
Bromide (Br^-)	0.03	ND*
Nitrite (NO_2^-)	0.23	ND*
Nitrate (NO_3^-)	63.85	2.38
Phosphate (PO_4^{3-})	2.98	ND*
Sulphate (SO_4^{2-})	58.35	0.07

* Not detectable

scavenge •OH [13]. The rate of oxidation of the probe C with •OH is described by Eq. (5) in which $k_{HO^{\bullet},C}$ is the second-order rate constant:

$$\frac{d[C]}{dt} = -k_{HO^{\bullet},C}[HO^{\bullet}]_{ss}[C] \quad (5)$$

Using a constant value for steady-state •OH concentration ($[HO^{\bullet}]_{ss}$) and integrating Eq. (5) yields:

$$ln\left(\frac{[C]_t}{[C]_0}\right) = -k_{HO^{\bullet},C}[HO^{\bullet}]_{ss}t = -k't \quad (6)$$

where k' (time^{-1}) is the pseudo-first order rate constant for carbamazepine degradation which can be measured experimentally. Since $k_{HO^{\bullet},C}$ is known, $[HO^{\bullet}]_{ss}$ can be determined. $[HO^{\bullet}]_{ss}$ in turn represents the ratio of •OH formation and the sum of its losses by reactions with scavengers, such as methanol. The rate of •OH generation through direct photolysis of water at 185 nm is given as:

$$\frac{d[HO^{\bullet}]}{dt} = \frac{\Phi_{H_2O,185nm} \times f_{H_2O,185nm} \times I_{0,185nm} \times A}{V} \quad (7)$$

where $\Phi_{H_2O,185nm}$ is the quantum yield of water photolysis at 185 nm and is equal to 0.33 [15], $f_{H_2O,185nm}$ is the fraction of 185 nm photons absorbed by water, $I_{0,185nm}$ is the incident photon fluence rate at 185 nm, A is the surface area of the irradiated sample (17.35 cm^2), and V is the volume of the solution (17 mL). In a solution composed of multiple solutes S, the rate of •OH consumption would be the sum of the rates of all reactions between •OH and S:

$$\frac{d[HO^{\bullet}]}{dt} = \sum k_{HO^{\bullet},S_i}[HO^{\bullet}]_{ss}[S_i] \quad (8)$$

Therefore, an expression for $[HO^{\bullet}]_{ss}$ is obtained by dividing Eq. (7) by Eq. (8):

$$[HO^{\bullet}]_{ss} = \frac{\Phi_{H_2O,185nm} \times f_{H_2O,185nm} \times I_{0,185nm} \times A}{V\sum k_{HO^{\bullet},S_i}[S_i]} \quad (9)$$

Combination of Eqs. (6) and (9) yields:

$$k' = \frac{k_{HO^{\bullet},C} \times \Phi_{H_2O,185nm} \times f_{H_2O,185nm)} \times I_{0,185nm} \times A}{V\sum k_{HO^{\bullet},S_i}[S_i]} \quad (10)$$

Carbamazepine (CBZ) and methanol (MeOH) were respectively used as probe (C) and model organic matter (S) with known second-order rate constants with •OH ($k_{HO^{\bullet},CBZ} = 6.8 \times 10^9$ M^{-1} s^{-1} and $k_{HO^{\bullet},MeOH} = 9.7 \times 10^8$ M^{-1} s^{-1}) [4,13]. Given the low concentrations of CBZ and MeOH used in the experiments compared to the concentration of water, water is considered as the main absorber of the VUV photons (i.e., $f_{H_2O,185nm} \approx 1$). As a result, Eq. (10) is simplified to:

$$k' = \frac{k_{HO^{\bullet},CBZ} \times \Phi_{H_2O,185nm} \times I_{0,185nm} \times A}{V \times k_{HO^{\bullet},MeOH} \times [MeOH]} = \frac{\Omega}{[MeOH]} \quad (11)$$

$$I_{0,185nm} = \frac{\Omega \times V \times k_{HO^{\bullet},MeOH}}{k_{HO^{\bullet},CBZ} \times \Phi_{H_2O,185nm} \times A} \quad (12)$$

This procedure allows for estimating the VUV fluence rate through experimental measurement of k' at different concentrations of methanol.

A VUV radiometer was used to measure the irradiance passing through the samples at 185 nm and determine the molar absorption coefficients of the solution components at this wavelength (Figure S2 and Section S3) [32]. For studying the effect of potable reuse water matrix on the advanced oxidation process (AOP) treatment, water samples were filtered with a 0.45 μm filter and spiked with 500 μg L^{-1} 1, 4-dioxane (1,4-D). The initial water quality parameters of the water samples are listed in Table 1.

2.3. Analytical methods

Free chlorine concentrations were measured using the DPD colorimetric method (Pocket Colorimeter™ II, Hach, USA). Concentrations of nitrobenzene (NB) and carbamazepine (CBZ) were quantified by high performance liquid chromatography (HPLC) (Thermo Scientific, USA) using a Dionex UltiMate 3000 system, equipped with a Nova-Pak C18 column (Waters Corp., USA). The injection volume was 100 μL and the mobile phase flow of 1.0 mL min^{-1} was composed of 30 % acetonitrile and 70 % water acidified to pH 2.5 with 10 mM phosphoric acid. UV detection of NB and CBZ was performed at 35°C at the wavelengths of 269 nm and 211 nm, respectively. Water samples containing 1,4-dioxane (1,4-D) were first extracted with dichloromethane (DCM) and the extracts were analyzed by gas chromatography/mass spectrometry (GC/MS, Shimadzu, USA) using a Shimadzu GC-2030/GCMS-QP2020 NX equipped with an SH-Rxi-5ms column (30 m × 0.25 mm ID × 0.25 μm film thickness). Details about sample preparation technique and analytical methods are provided in Section S4.

To study the effect of pH, the pH of samples buffered with 2 mM phosphate buffer was adjusted to various values. pH was measured by an Oakton pH meter calibrated at pH 4, 7, and 10 with a disposable type gel filled probe.

3. Results and discussion

3.1. Measuring the incident fluence rate at 185 nm

Fig. 1(a) shows the experimental measurement of k' for photodegradation of CBZ at different concentrations of MeOH. Plotting the k' values versus $\frac{1}{[MeOH]}$ helps determine the parameter Ω and consequently $I_{0,185nm}$ by using Eq. (12) (Fig. 1(b)). The average 185 nm incident fluence rate, $I_{0,185nm}$, after applying the correction factors was estimated as 0.071 ± 0.002 mW cm^{-2}. Using the average 254 nm fluence rate in the same apparatus, determined by chemical actinometry, the lamp output ratio of VUV 185 nm to UV 254 nm was estimated as ~12 % on an energy basis. This ratio is in agreement with the range of 10–30 % reported by Barnes [1] and Johnson [19], who used different types of low pressure mercury lamps.

For consistency of the results with existing literature, all UV fluence values throughout the rest of the paper are reported based on UV 254 nm, which allows for a better comparison with other research and serves as a reference in industry.

3.2. Micropollutant removal in the VUV/UV/Cl_2 process

Photodegradation of CBZ and 1,4-D were investigated using the VUV/UV, VUV/UV/Cl_2, and UV/Cl_2 processes and the results are presented in Fig. 2(a) and (b). Removal of both contaminants is negligible under either UV irradiation alone (i.e., 254 nm light) or dark chlorination due to the lack of reactive species to oxidize the micropollutants. In contrast, both VUV/UV and VUV/UV/Cl_2 processes yielded significantly higher removal rates compared to the UV/Cl_2 process primarily due to the direct photolysis of water molecules at 185 nm which generates additional amounts of •OH contributing to the degradation of CBZ and 1,4-D. It should be noted that VUV/UV direct photolysis of most micropollutants, including CBZ and 1,4-D, is unlikely due to their lack of chromophores to absorb VUV/UV photons, and their low concentrations relative to water (i.e., ~55.5 M), which allows them to absorb only a negligible fraction of photons [43]. Therefore, water would remain the primary absorber of the 185 nm photons in VUV/UV reactions and it is safe to assume that no photons directly act on either of the contaminants [54]. Comparing the results of VUV/UV and VUV/UV/Cl_2 suggests that addition of 70 μM free chlorine (5.0 mg Cl_2 L^{-1}) to the VUV/UV AOP only slightly improves the removal rate of CBZ by ~12 % (p-value (t-test) > 0.05; i.e., while the improvement is observable, it is not statistically significant) while slowing down the degradation of 1,4-D by ~50 % compared to the VUV/UV AOP. It has been previously shown that in the VUV/UV AOP, free chlorine exhibits a dual role: (i)

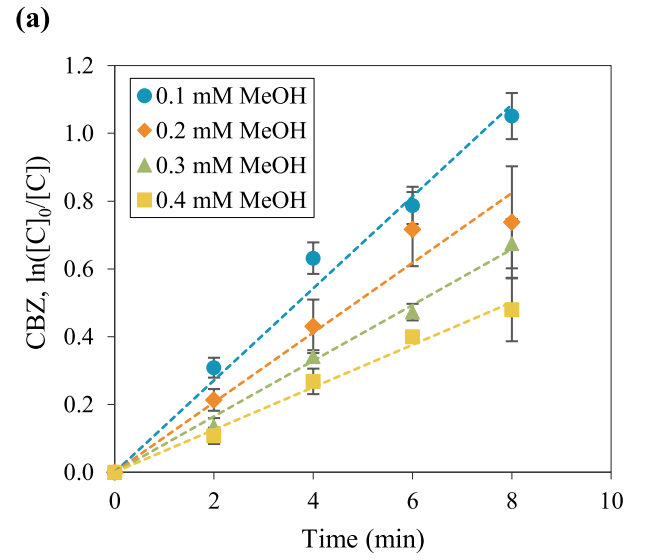

[MeOH] = 0.1 mM	[MeOH] = 0.2 mM	[MeOH] = 0.3 mM	[MeOH] = 0.4 mM
y = 0.14x	y = 0.10x	y = 0.08x	y = 0.06x
R^2 = 0.99	R^2 = 0.99	R^2 = 0.99	R^2 = 0.99

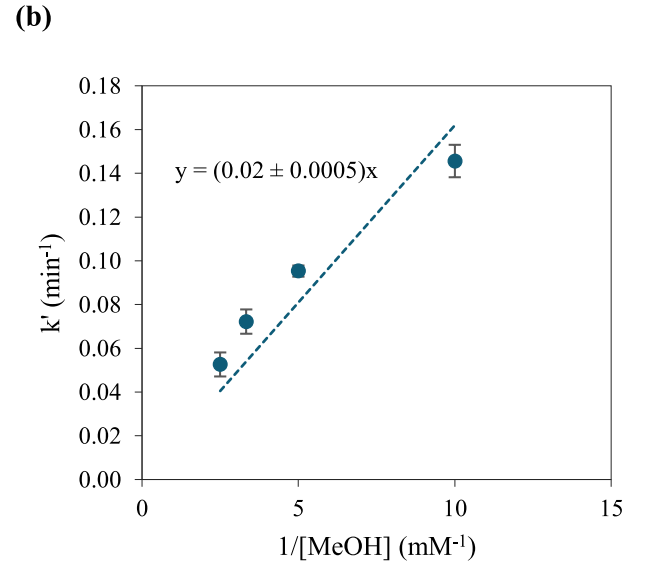

Fig. 1. (a) Experimental measurement of the pseudo-first order photodegradation rate constant of CBZ at different concentrations of MeOH ($[C]_{CBZ,0}$ = 0.85 μM); (b) Estimation of the incident fluence rate at 185 nm based on the experimental results of CBZ degradation in presence of MeOH. Error bars represent the standard deviations of three experimental replicates.

promoting the process as a result of radical generation (•OH and Cl•) through direct photolysis reactions at both 254 nm and 185 nm [6,12,28,32]; (ii) inhibiting the treatment process by competing for photons ($\varepsilon_{HOCl,185nm}$ = 3900 M^{-1} cm^{-1} and $\varepsilon_{OCl^-,185nm}$ = 4700 M^{-1} cm^{-1} corresponding to ~15 % absorption of the VUV emission at a chlorine dose of 70 μM) and radicals (Eqs. 13 – 16). The latter effect partly inhibits •OH production through direct photolysis of water and also reduces the availability of radicals for contaminant degradation [32].

$$HOCl + HO^{\bullet} \rightarrow ClO^{\bullet} + H_2O \qquad k = 2.0 \times 10^9\ M^{-1}s^{-1} \tag{13}$$

$$HOCl + Cl^{\bullet} \rightarrow ClO^{\bullet} + HCl \qquad k = 3.0 \times 10^9\ M^{-1}s^{-1} \tag{14}$$

$$OCl^- + HO^{\bullet} \rightarrow ClO^{\bullet} + OH^- \qquad k = 8.8 \times 10^9\ M^{-1}s^{-1} \tag{15}$$

$$OCl^- + Cl^{\bullet} \rightarrow ClO^{\bullet} + Cl^- \qquad k = 8.3 \times 10^9\ M^{-1}s^{-1} \tag{16}$$

In addition, the different reactivities of CBZ and 1,4-D with •OH and Cl• directly influence their degradation rates in the VUV/UV/Cl_2 and VUV/UV AOPs. In the case of CBZ, the opposing effects of radical generation and scavenging nearly offset one another, as the high reaction rates with both •OH and Cl• ($k_{HO^{\bullet},CBZ}$ = 6.8 × 10^9 M^{-1} s^{-1} and $k_{Cl^{\bullet},CBZ}$ = 6.6 × 10^{10} M^{-1} s^{-1} [32]) maintain a consistent removal rate across both AOPs. On the other hand, 1,4-D exhibits significantly lower reactivity with Cl• compared to •OH ($k_{HO^{\bullet},1,4-D}$ = 6.8 × 10^9 M^{-1} s^{-1} and $k_{Cl^{\bullet},1,4-D}$ = 4.4 × 10^6 M^{-1} s^{-1} [38]). Therefore, the Cl• generated through direct photolysis of free chlorine does not significantly enhance 1,4-D removal; instead, the degradation rate of 1,4-D is mainly controlled by photon shielding and radical scavenging effects. The performance of each AOP in removing CBZ and 1,4-D is summarized in Table 2.

Other studies on micropollutant degradation in a VUV/UV/Cl_2 process suggest that the varying effects of free chlorine on a VUV/UV process may not be limited only to the ones discussed here. In fact, the type of micropollutant of concern might also play a role and result in a different removal rate from the ones obtained in this study. For instance, Li et al. [25,28] have shown that the photodegradation rate of methylene blue and sulfamethazine are respectively increased by 4.4-fold and 1.7-fold when free chlorine is added to the VUV/UV AOP.

3.3. Effect of free chlorine dose

The effect of free chlorine dose on CBZ and 1,4-D degradation was studied at four chlorine levels (50 – 200 μM) and the results are shown in Fig. 3(a) and (b). In the case of CBZ, addition of up to 200 μM chlorine did not impact the degradation (p-value (*t*-test) > 0.05; i.e., statistically insignificant). For 1,4-D, on the other hand, all the studied chlorine levels slowed down the removal rate in the VUV/UV/Cl_2 AOP with almost complete inhibition (i.e., ~95 %) at a chlorine dose of 200 μM (p-value (*t*-test) < 0.05). Although an improved degradation is expected because of the formation of additional amounts of reactive radicals during the direct photolysis of chlorine species, the reactivity of the studied micropollutants with the produced RCS also affects the treatment and needs to be considered. As discussed earlier, high reactivity of CBZ with Cl• ($k_{Cl^{\bullet},CBZ}$ = 6.6 × 10^{10} M^{-1} s^{-1}) promised an increased degradation rate, in line with the observations made by Xiao et al. [50] for the removal of dodecyl dimethyl benzyl ammonium chloride in the VUV/UV/Cl_2 AOP. Yet, 1,4-D degradation was reduced by the presence of chlorine because of its low reactivity with Cl• ($k_{Cl^{\bullet},1,4-D}$ = 4.4 × 10^6 M^{-1} s^{-1}) and scavenging of •OH by free chlorine species. The radical scavenging effect is more likely the prominent cause of this observation. Despite the low reactivity of Cl• with 1,4-D, it can be indirectly converted to •OH (Eqs. 17 and 18) [18,21]. However, even with this conversion, no significant improvement in 1,4-D removal was achieved. This suggests that the overall impact of radical generation from chlorine photolysis is minimal compared to other inhibitory mechanisms at play.

$$Cl^{\bullet} + OH^- \rightarrow HClO^{\bullet -} \qquad k = 1.8 \times 10^{10}\ M^{-1}s^{-1} \tag{17}$$

$$HClO^{\bullet -} \rightarrow Cl^- + HO^{\bullet} \qquad k = 6.1 \times 10^9\ s^{-1} \tag{18}$$

As mentioned earlier, free chlorine species exhibit a high absorption coefficient at 185 nm ($\varepsilon_{HOCl,185nm}$ = 3900 M^{-1} cm^{-1}, $\varepsilon_{OCl^-,185nm}$ = 4700 M^{-1} cm^{-1}, and $\varepsilon_{water,185nm}$ = 0.032 M^{-1} cm^{-1}) [15,32]. Therefore, one potential inhibitive mechanism is that hypochlorous acid (HOCl) and hypochlorite ion (OCl^-) in the water matrix act as inner filters, blocking a portion of the incident VUV photons. This reduces the generation of •OH through direct photolysis of water under VUV/UV irradiation. Furthermore, free chlorine species are potential scavengers of reactive radicals, including •OH and Cl•, as shown in Eqs. (13) – (16) [7,21,33]. The rates of these scavenging reactions are comparable to those

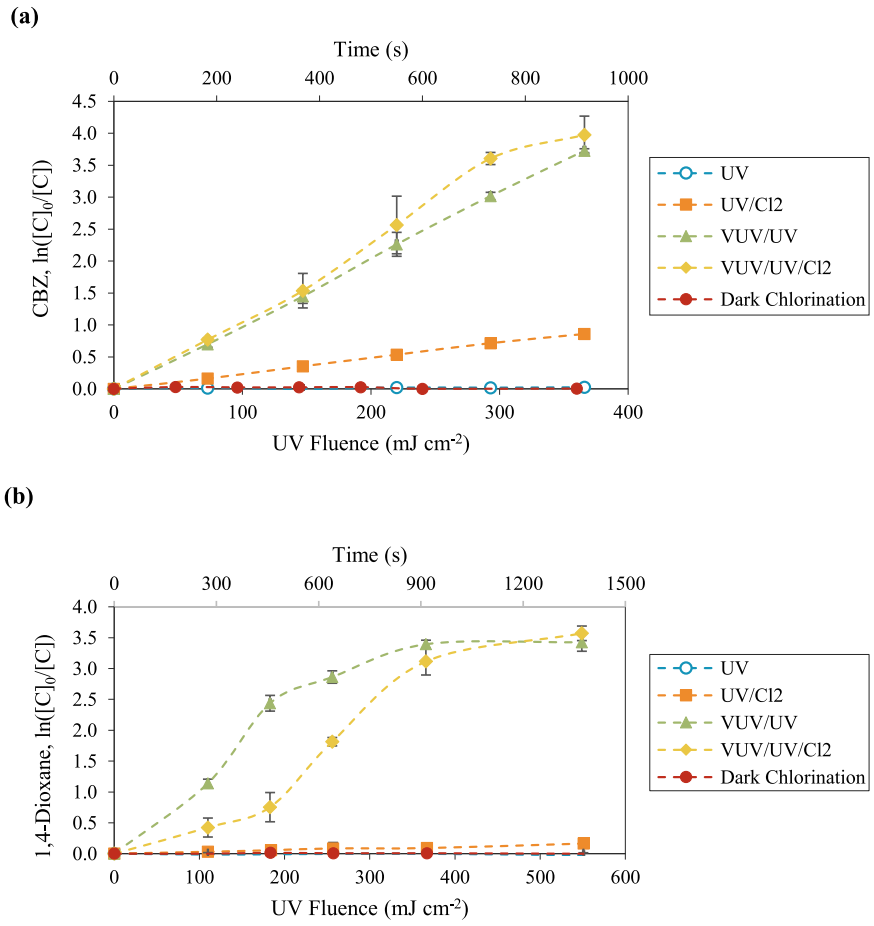

Fig. 2. Degradation of (a) CBZ and (b) 1,4-D under different AOP conditions in DI water ($[C]_{CBZ,0}$ = 4 μM, $[C]_{1,4\text{-}D,0}$ = 6 μM, $[C]_{free\ chlorine,0}$ = 70 μM, Average pH = 6.5 (unadjusted)). Error bars represent the standard deviations of three experimental replicates.

Table 2
Removal of CBZ and 1,4-D by UV, UV/Cl_2, VUV/UV, and VUV/UV/Cl_2 processes.

Advanced Oxidation Process	CBZ	1,4-D
UV	2.44 %	0.00 %
UV/Cl_2	57.63 %	15.17 %
VUV/UV	97.59 %	96.75 %
VUV/UV/Cl_2	98.12 %	97.19 %

of micropollutant degradation by $^{\bullet}OH$ and $Cl^{\bullet}$ (typically ~10^8 – 10^{10} M^{-1} s^{-1}). Therefore, high concentrations of free chlorine species compete with CBZ and 1,4-D for available reactive radicals, thereby reducing the rates of micropollutant removal by consuming the generated $^{\bullet}OH$ and $Cl^{\bullet}$.

Fig. 3(b) also shows an inflection point in the degradation rates of 1,4-D in the VUV/UV/Cl_2 AOP. Monitoring the residual chlorine concentration in the irradiated samples revealed that for chlorine doses of 50 – 100 μM, free chlorine depletes in the solution at a UV fluence of ~250 mJ cm^{-2} leaving no detectable residual in the water matrix. At this point, the photodegradation rate of 1,4-D is accelerated as there are no more interferences due to the presence of chlorine species in the solution (Figure S3).

3.4. Effect of pH

Photodegradation rates of CBZ and 1,4-D in the VUV/UV/Cl_2 AOP were compared at three environmentally relevant pH levels (Fig. 4). In general, solution pH can affect micropollutant removal in AOP systems by changing the protonated/deprotonated forms of the target contaminant and some scavengers, as well as affecting oxidant speciation and therefore radical generation [53]. Here, control experiments without addition of free chlorine oxidant revealed that the VUV/UV photodegradation of neither CBZ nor 1,4-D is significantly affected by the changes in solution pH (Figures S4 and S5); therefore, pH variations within the range of 4.0 – 9.5 are assumed to be only related to radical chemistry involving chlorine.

Free chlorine species mainly consist of HOCl or OCl^- which are distributed in the solution as a function of pH (Eq. 19) [17]:

$$HOCl \longleftrightarrow H^+ + OCl^- \qquad pK_a = 7.5 \tag{19}$$

This indicates that HOCl is the main chlorine species at pH < 7.5, while OCl^- predominates at pH > 7.5 and any change in the solution pH results in an inter-conversion of these two species.

In the VUV/UV/Cl_2 AOP, the observed pseudo-first order rate constants for the degradation of both CBZ and 1,4-D were significantly decreased with increasing pH from 4.0 to 9.5. The impact of free chlorine on radical generation and scavenging varies with pH, primarily due to differences in photon absorption and reactivity between HOCl and OCl^-. Considering the dissociation of free chlorine, a few reasons are presented to explain this observed trend. First, under alkaline pH conditions where OCl^- is the dominant chlorine species, a greater portion of the incident VUV photons is blocked compared to the solutions at lower pH levels. The molar absorption coefficients of HOCl and OCl^- at 185 nm are reported as 3900 $M^{-1}cm^{-1}$ and 4700 M^{-1} cm^{-1}, respectively [32]. This increased absorption inhibits the direct photolysis of water molecules more effectively in the presence of OCl^-, leading to reduced $^{\bullet}OH$ generation for reacting with micropollutants. Second, variations in

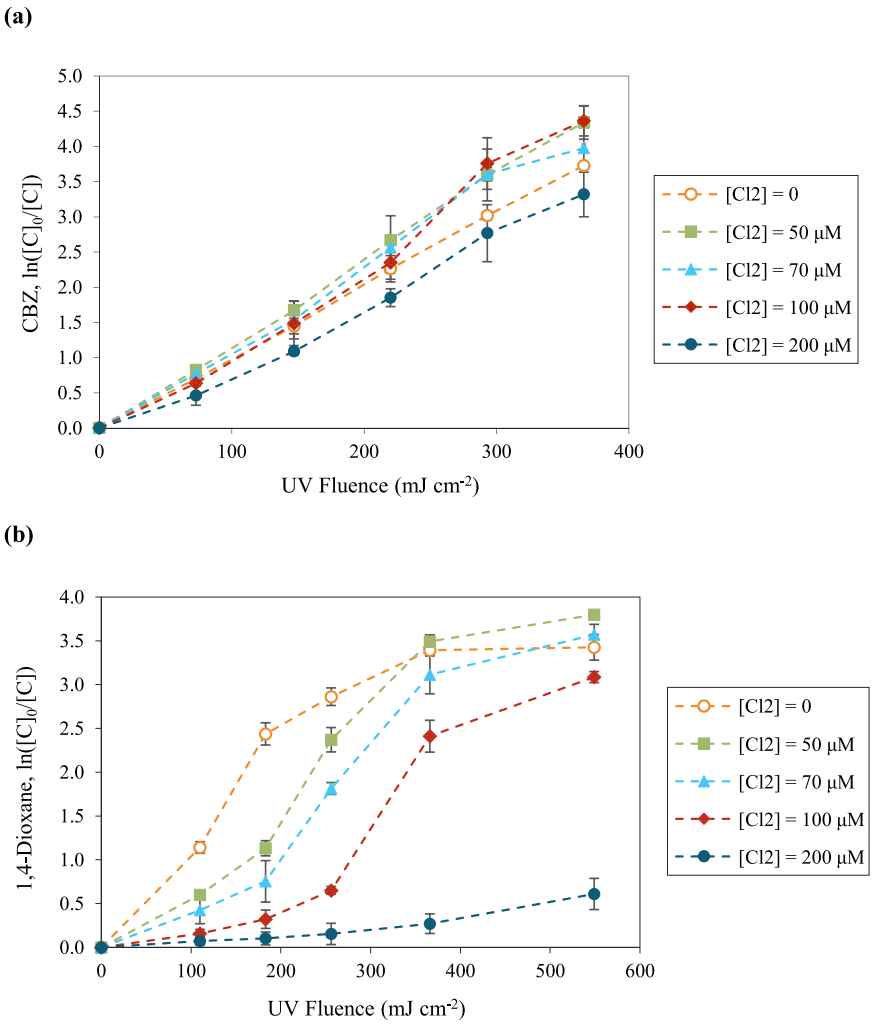

Fig. 3. Effect of free chlorine dose on the VUV/UV AOP for degradation of (a) CBZ, and (b) 1,4-D in DI water ($[C]_{CBZ,0}$ = 4 µM, $[C]_{1,4\text{-}D,0}$ = 6 µM, Average pH = 6.5 (unadjusted)). Error bars represent the standard deviations of three experimental replicates.

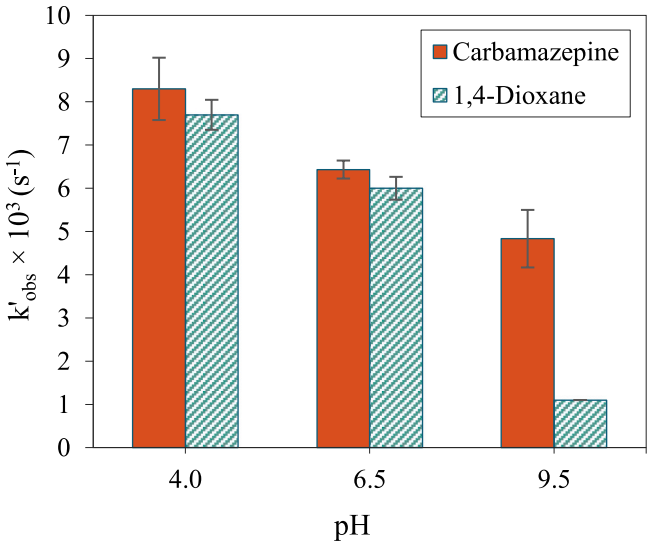

Fig. 4. Observed pseudo-first order rate constants for the degradation of CBZ and 1,4-D in the VUV/UV/Cl_2 AOP in DI water as a function of pH ($[C]_{CBZ,0}$ = 4 µM, $[C]_{1,4\text{-}D,0}$ = 6 µM, $[C]_{free\ chlorine,0}$ = 70 µM, $[C]_{phosphate\ buffer}$ = 2 mM). Error bars represent the standard deviations of three experimental replicates.

solution pH also affect the quantum yield of free chlorine, influencing radical formation. Previous studies have shown that the direct photolysis of HOCl under both 254 nm and 185 nm radiations occur with a higher quantum yield compared to OCl^- as it was shown in Eqs. (3) and (4) [8,32]. Thus, lower pH levels (e.g., pH 4 and 6.5) enhance HOCl's ability to generate reactive radical species, resulting in higher degradation rates of micropollutants.

Also, HOCl and OCl^- scavenge the reactive radicals with different rate constants as it was shown in Eqs. (13) – (16). OCl^- consumes both $^{\bullet}OH$ and $Cl^{\bullet}$ more rapidly compared to HOCl which further inhibits the degradation of micropollutants at higher pH levels.

Fig. 4 also shows that the rate of 1,4-D photodegradation is more significantly affected by an increase in pH compared to CBZ. As discussed earlier, this can be attributed to the production of $Cl^{\bullet}$ and inhibition of $^{\bullet}OH$ generation through direct photolysis reactions at pH 9.5. Given the lower rate constant of 1,4-D with $Cl^{\bullet}$ as compared to that of CBZ ($k_{Cl^{\bullet},1,4-D} = 4.4 \times 10^6\ M^{-1}\ s^{-1}$ and $k_{Cl^{\bullet},CBZ} = 6.6 \times 10^{10}\ M^{-1}\ s^{-1}$), alkaline pH imposes a more intensive inhibitory effect on 1,4-D degradation in the VUV/UV/Cl_2 AOP.

3.5. Competition kinetics and contribution of radicals

To further understand the kinetics of radical reactions, the rates of micropollutant degradation were monitored in the presence of 0.4 mM t-BuOH and 40 µM NB as radical scavengers in the VUV/UV/Cl_2 AOP

($k_{HO^\bullet,t-BuOH}$ = 6.0 × 10^8 M^{-1} s^{-1}, $k_{Cl^\bullet,t-BuOH}$ = 3.0 × 10^8 M^{-1} s^{-1}, $k_{HO^\bullet,NB}$ = 3.9 × 10^9 M^{-1} s^{-1}) [4,34]. t-BuOH effectively scavenges $^\bullet$OH and $Cl^\bullet$, thereby eliminating their impact on the degradation of CBZ or 1,4-D. This allows for observing the potential effect of $Cl_2^{\bullet-}$ only. Similarly, NB selectively reacts with $^\bullet$OH, enabling the observation of the contributions of $Cl^\bullet$ and $Cl_2^{\bullet-}$ to micropollutants removal. By comparing the observed pseudo-first order rate constants obtained in the VUV/UV/Cl_2 AOPs with and without the presence of radical scavengers, it is possible to estimate the contribution of each radical species to the degradation of CBZ and 1,4-D (Fig. 5).

Given the non-selective nature of $^\bullet$OH and the fact that direct photolysis of water molecules – as the primary absorber of the incident 185 nm photons – generates abundant amounts of $^\bullet$OH in the solution, it is observed that $^\bullet$OH dominates the elimination reactions of both CBZ and 1,4-D. Reactive chlorine species (RCSs), including $Cl^\bullet$ and $Cl_2^{\bullet-}$, are generally more selective than $^\bullet$OH and tend to react preferentially with electron-rich moieties in CBZ and 1,4-D molecules [29]. However, because of the slower reaction rate of $Cl^\bullet$ with 1,4-D compared to that of CBZ, $Cl^\bullet$ does not significantly contribute to the degradation of 1,4-D. On the other hand, $Cl_2^{\bullet-}$ has been reported to react with CBZ and 1,4-D with second order rate constants of 4.30 × 10^7 M^{-1} s^{-1} and 3.30 × 10^6 M^{-1} s^{-1}, respectively [24,38]; however, competition kinetic experiments indicate that $Cl_2^{\bullet-}$ contributes almost identically to the degradation of CBZ and 1,4-D in the VUV/UV/Cl_2 AOP. These experimental observations are in agreement with the reported reactivity of $Cl_2^{\bullet-}$ in the literature which has also been confirmed with the aid of kinetic modelling [29,38,39]. Yet, more accurate predictions of the fate of RCS and their contribution to micropollutants degradation can be made through a comprehensive kinetic model and use of other probe/scavenger compounds.

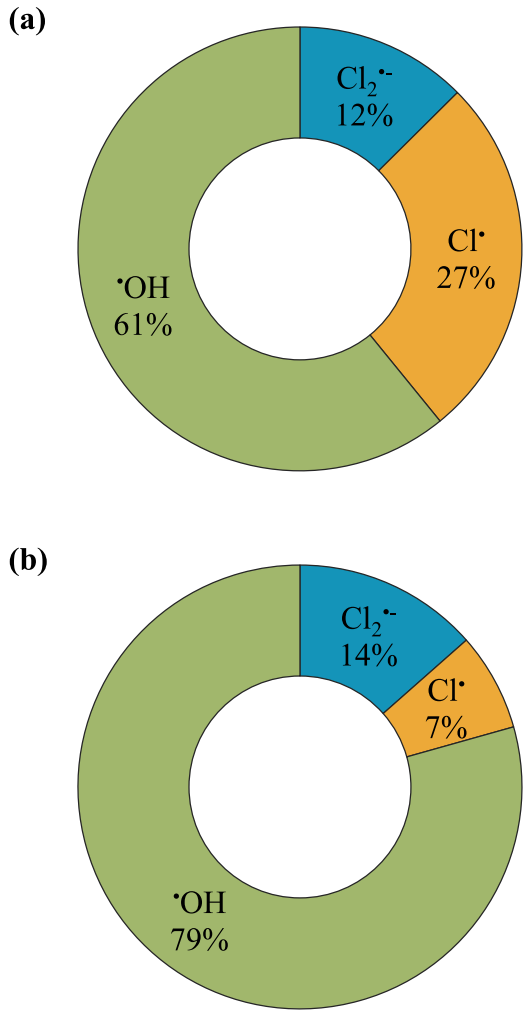

Fig. 5. Contribution of $^\bullet$OH, $Cl^\bullet$, and $Cl_2^{\bullet-}$ to the degradation of (a) CBZ and (b) 1,4-D in the VUV/UV/Cl_2 AOP in DI water ($[C]_{CBZ,0}$ = 4 μM, $[C]_{1,4\text{-}D,0}$ = 6 μM, $[C]_{free\ chlorine,0}$ = 70 μM, $[C]_{t\text{-}BuOH}$ = 0.4 mM, $[C]_{NB}$ = 40 μM, Average pH = 6.5 (unadjusted)).

3.6. Effect of potable reuse water matrix

Photodegradation of 1,4-D in the VUV/UV and VUV/UV/Cl_2 AOPs was investigated in water samples taken from O_3/BAC effluent and RO permeate at potable reuse facilities, and the results were compared with the ones obtained in a DI water matrix (Fig. 6). As it is shown in Table 1, in case of the O_3/BAC effluent, the presence of different solutes including alkalinity, dissolved organic carbon (DOC), and ions makes the water matrix a lot more complicated than DI water and leads to variations in optical properties at 185 nm. It is expected that even under such conditions, water remains the primary absorber of the 185 nm photons due to its very high concentration (i.e., ~55.5 M); however, the high absorption coefficients of water solutes in the VUV range limits the penetration of 185 nm photons in the solution and reduces the treatment efficiency of 1,4-D in the O_3/BAC effluent matrix (Fig. 6(a)). Previous studies have measured the molar absorption coefficients at 185 nm for alkalinity (as bicarbonate ion), DOC (as natural organic matter), chloride, nitrate, and sulphate and reported these values at 290 M^{-1} cm^{-1}, 1402 M^{-1} cm^{-1}, 3063 M^{-1} cm^{-1}, 4779 M^{-1} cm^{-1}, and 146 M^{-1} cm^{-1}, respectively [14,37]. The high absorbances at 185 nm imply that all water solutes scavenge a portion of the incident VUV photons (Table S1) and thereby inhibit formation of $^\bullet$OH through water photolysis. In addition, alkalinity, DOC, and chloride also impact the AOP reactions through scavenging the reactive $^\bullet$OH and therefore reducing the amount of available reactive agents for micropollutant removal ($k_{HO^\bullet,HCO_3^-}$ = 8.5 × 10^6 M^{-1} s^{-1}, $k_{Cl^\bullet,HCO_3^-}$ = 2.2 × 10^8 M^{-1} s^{-1}, $k_{HO^\bullet,DOC}$ ~ 10^8 M^{-1} s^{-1}, $k_{Cl^\bullet,DOC}$ ~ 10^8 M^{-1} s^{-1}, $k_{HO^\bullet,Cl^-}$ = 4.3 × 10^9 M^{-1} s^{-1}, $k_{Cl^\bullet,Cl^-}$ = 8.5 × 10^9 M^{-1} s^{-1}) [4,5,18,41,45]. Although bicarbonate and sulphate ions have been reported to undergo direct photolysis reactions to produce $CO_3^{\bullet-}$ and $SO_4^{\bullet-}$ species, they are highly specific compared to the non-specific $^\bullet$OH and $Cl^\bullet$; therefore, the reactivities of $CO_3^{\bullet-}$ and $SO_4^{\bullet-}$ were not considered in this study for the removal of 1,4-D [2,9]. Consequently, as it is shown in Fig. 6(a), the degradation kinetics of 1,4-D in both VUV/UV and VUV/UV/Cl_2 AOPs are significantly slower in the O_3/BAC water matrix compared to those in DI water. Yet, the addition of free chlorine oxidant slightly improved the treatment efficiency for the VUV/UV/Cl_2 in the O_3/BAC effluent. This could be due to the potential formation of RCSs, $Cl^\bullet$ and $Cl_2^{\bullet-}$, as a result of direct photolysis and subsequent secondary reactions with chloride ions (Cl^-) in the water matrix according to Eq. (20). Cl^- in the O_3/BAC water matrix acts as a promotive agent for the formation of large amounts of $Cl_2^{\bullet-}$, which plays an important role in 1,4-D degradation based on the previous discussion on competition kinetic results (Fig. 5(b)).

$$Cl^\bullet + Cl^- \rightarrow Cl_2^{\bullet-} \qquad k = 8.5 \times 10^9\ M^{-1}s^{-1} \tag{20}$$

$$NH_2Cl \xrightarrow{h\nu} NH_2^\bullet + Cl^\bullet \qquad \Phi_{254nm} = 0.24 \tag{21}$$

$$NHCl_2 \xrightarrow{h\nu} NHCl^\bullet + Cl^\bullet \qquad \Phi_{254nm} = 1.77 \tag{22}$$

In potable reuse trains which include membrane processes, chloramines (NH_2Cl and $NHCl_2$) are either added or generated in situ in the water upstream of RO treatment to mitigate biofouling on membrane surfaces [23]. Chloramines can then pass through the RO system and appear in the AOP treatment, where they can potentially affect the process efficiency either by scavenging photon and radicals or through direct photolysis reactions [8,31]. As RO removes almost all water constituents to a great extent, the relatively clear matrix of the RO permeate favors the faster degradation kinetics of 1,4-dioxane (Fig. 6

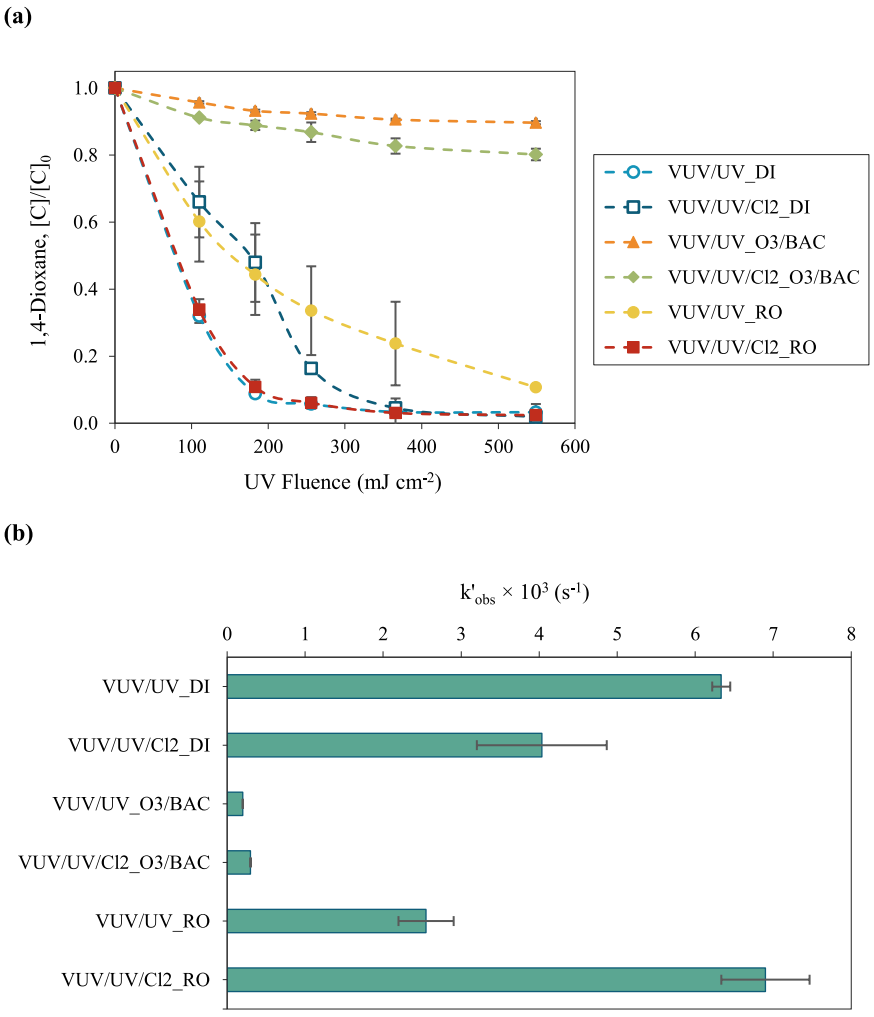

Fig. 6. (a) Degradation kinetics of 1,4-D in the VUV/UV and VUV/UV/Cl2 AOPs obtained in water samples from potable reuse trains as compared to DI water and (b) Comparison of the pseudo-first order rate constants for 1,4-D degradation in the VUV/UV and VUV/UV/Cl2 AOPs in different water matrices ($[C]_{1,4\text{-}D,0}$ = 6 μM, $[C]_{free\ chlorine,0}$ = 70 μM). Error bars represent the standard deviations of three and two experimental replicates for DI water and the investigated water samples, respectively.

(a)). With the VUV/UV AOP, the rate of 1,4-dioxane removal in the RO permeate was almost half of the rate obtained in DI water, potentially due to the small amounts of alkalinity, DOC, chloride, and nitrate ions which are all great scavengers of the reactive agents (Fig. 6(b)). Under such conditions, it seems that the effect of chloramine photolysis is negligible compared to the photon and radical scavenging effects. On the other hand, the results showed that addition of free chlorine oxidant to the RO permeate improves the rate of 1,4-dioxane removal in the VUV/UV/Cl_2 AOP. This can be attributed to the simultaneous direct photolysis of both free chlorine and chloramines in the VUV/UV/Cl_2 AOP (Eqn 3, 4, 21 and 22) resulting in an augmentation of $Cl^{\bullet}$ during the treatment. The excess $Cl^{\bullet}$ can then react with Cl^- as shown in Eq. (20) to produce $Cl_2^{\bullet-}$ [31]. This pathway potentially benefits the treatment by providing large amounts of two different reactive agents, $Cl^{\bullet}$ and $Cl_2^{\bullet-}$, in addition to the existing $^{\bullet}OH$. The suggested mechanism seems to outweigh the photon and radical scavenging reactions by background species in a relatively clean water matrix such as RO permeate and therefore clearly explains the observed 1,4-D degradation kinetics in the VUV/UV and VUV/UV/Cl_2 AOPs.

The current approach in potable reuse trains is to implement a UV-based AOP following the RO treatment. The standard oxidants that are widely used in practice for the AOPs include hydrogen peroxide (H_2O_2) and free chlorine [29]. Here, the proposed VUV/UV and VUV/UV/Cl_2 processes were compared to the existing UV AOPs for treatment of 1,4-D in the RO permeate water matrix. Among the studied AOPs, UV/Cl_2 exhibited the least efficiency for 1,4-D degradation (Figure S6). Furthermore, the treatment efficiency of UV/H_2O_2 in the RO permeate matrix was found to be almost the same as VUV/UV AOP (Figure S6); however, VUV/UV remains superior as an oxidant-free process which eliminates the need for adding H_2O_2 as well as quenching the residual H_2O_2 after the treatment. Finally, as it was discussed earlier, the VUV/UV/Cl_2 demonstrated the fastest removal rate for 1,4-D in RO permeate compared to VUV/UV AOP due to the formation of $Cl_2^{\bullet-}$ which readily contributes to the degradation process.

The results from testing potable reuse matrices also suggest that scaling VUV-based AOPs to full-scale systems may face operational challenges due to the limited penetration of VUV photons in water containing dissolved solutes [52]. Therefore, designing effective full-scale photochemical reactors will require optimizing lamp spacing, improving hydrodynamic conditions, and implementing automatic cleaning mechanisms to manage fouling – all crucial for maintaining treatment efficiency. Future research should continue to explore these aspects to further support the development of VUV AOPs in water treatment and potable reuse systems.

4. Conclusions

Previous research on the VUV/UV/Cl_2 AOP has highlighted the

synergistic effect of RCS and $^{\bullet}OH$ for micropollutant degradation. In this study, the performance of VUV/UV/Cl_2 was evaluated and compared with VUV/UV alone for eliminating CBZ and 1,4-D as model organic contaminants in potable reuse trains. Under potable reuse conditions, the addition of free chlorine to the VUV/UV AOP roughly maintained CBZ degradation levels while reducing the rate of 1,4-D removal due to potential $^{\bullet}OH$ and $Cl^{\bullet}$ scavenging by chlorine species. The VUV/UV/Cl_2 AOP exhibited effective treatment performance under relevant chlorine doses and pH conditions for potable reuse scenarios. In RO-based potable reuse systems, VUV/UV/Cl_2 demonstrated efficient 1,4-D degradation due to the relatively clear water matrix and potential synergies between added free chlorine and existing chloramine species, facilitating $Cl_2^{\bullet-}$ generation – the primary RCS contributing to 1,4-D removal.

Further research is needed to determine the interaction mechanisms between free chlorine and chloramines in the RO permeate matrix and to incorporate the effects of other matrix components on the VUV/UV AOP. Although free chlorine alone might not have the capacity to improve the degradation of a wide range of organic contaminants in a VUV/UV AOP, implications of combining free chlorine with other oxidants, such as chloramines, can be considered for advancing a viable VUV/UV AOP.

Funding sources

This research was financially supported by the Natural Sciences and Engineering Research Council of Canada (NSERC).

CRediT authorship contribution statement

Madjid Mohseni: Writing – review & editing, Supervision, Resources, Funding acquisition, Conceptualization. **William Mitch:** Writing – review & editing. **Mahsa Masjoudi:** Writing – original draft, Methodology, Investigation, Data curation, Conceptualization. **Benoit Barbeau:** Writing – review & editing. **Fuhar Dixit:** Writing – review & editing, Investigation.

Declaration of Competing Interest

The authors declare that they have no known competing financial interests or personal relationships that could have appeared to influence the work reported in this paper.

Acknowledgements

Fuhar Dixit is a Natural Sciences and Engineering Research Council of Canada's (NSERC) postdoctoral Scholar at The University of California Berkeley and a former Michael Smith Foreign Study Supplement Fellow at Stanford University. Sincere thanks to Professor Naoko Ellis from the UBC Chemical and Biological Engineering Department for assisting with the 1,4-D analysis, Professor Karl Linden (Department of Civil and Environmental Engineering, University of Colorado, Boulder), Professor Tzahi Cath (Department of Civil and Environmental Engineering, Colorado School of Mines) and Stephanie S. Lau (Department of Civil and Environmental Engineering, Stanford University) for supplying the water samples used in this study.

Author Contributions

The manuscript was written through contributions of all authors. All authors have given approval to the final version of the manuscript.

Appendix A. Supporting information

Supplementary data associated with this article can be found in the online version at doi:10.1016/j.jece.2024.115095.

Data availability

Data will be made available on request.

References

[1] B.T. Barnes, Intensities of λ1850 and λ2537 in low-pressure mercury vapor lamps with rare gas present, J. Appl. Phys. 31 (1960) 852–854.
[2] J. Barrett, M.F. Fox, A.L. Mansell, The photochemistry of aqueous sulfate ion, J. Phys. Chem. 69 (1965) 2996–3000.
[3] J.R. Bolton, K.G. Linden, Standardization of methods for fluence (UV dose) determination in bench-scale UV experiments, J. Environ. Eng. 129 (2003) 209–215, https://doi.org/10.1061/(ASCE)0733-9372(2003)129:3(209).
[4] G.V. Buxton, C.L. Greenstock, W.P. Helman, A.B. Ross, Critical review of rate constants for reactions of hydrated electrons, hydrogen atoms and hydroxyl radicals (· OH/· O− in aqueous solution, J. Phys. Chem. Ref. data 17 (1988) 513–886, https://doi.org/10.1063/1.555805.
[5] G.V. Buxton, M. Bydder, G.A. Salmon, Reactivity of chlorine atoms in aqueous solution Part 1The equilibrium Cl MNsbd+ Cl-Cl 2, J. Chem. Soc. Faraday Trans. 94 (1998) 653–657, https://doi.org/10.1039/A707377A.
[6] G.V. Buxton, M.S. Subhani, Radiation chemistry and photochemistry of oxychlorine ions. Part 2.—Photodecomposition of aqueous solutions of hypochlorite ions, J. Chem. Soc. Faraday Trans. 1 Phys. Chem. Condens. Phases 68 (1972) 958–969, https://doi.org/10.1039/F19726800958.
[7] G.V. Buxton, M.S. Subhani, Radiation chemistry and photochemistry of oxychlorine ions. Part 1.—Radiolysis of aqueous solutions of hypochlorite and chlorite ions, J. Chem. Soc. Faraday Trans. 1 Phys. Chem. Condens. Phases 68 (1972) 947–957, https://doi.org/10.1039/F19726800947.
[8] Y.H. Chuang, S. Chen, C.J. Chinn, W.A. Mitch, Comparing the UV/monochloramine and UV/free chlorine advanced oxidation processes (AOPs) to the UV/hydrogen peroxide AOP under scenarios relevant to potable reuse, Environ. Sci. Technol. 51 (2017) 13859–13868, https://doi.org/10.1021/acs.est.7b03570.
[9] F.S. Dainton, P. Fowles, The photolysis of aqueous systems at 1849 Å II. Solutions containing Cl-, Br-, SO2-4 or OH-ions, Proc. R. Soc. Lond. Ser. A. Math. Phys. Sci. 287 (1965) 312–327, https://doi.org/10.1098/rspa.1965.0182.
[10] J. Fang, Y. Fu, C. Shang, The roles of reactive species in micropollutant degradation in the UV/free chlorine system, Environ. Sci. Technol. 48 (2014) 1859–1868, https://doi.org/10.1021/es4036094.
[11] L. Farkas, I. Monzini, E. Takacs, L. Wojnarovits, M. Voros, C. Vagvolgyi, C. Janaky, T. Alapi, Comparison of the effectiveness of UV, UV/VUV photolysis, ozonation, and ozone/UV processes for the removal of sulfonamide antibiotics, J. Environ. Chem. Eng. 12 (2024) 111845, https://doi.org/10.1016/j.jece.2023.111845.
[12] Y. Feng, D.W. Smith, J.R. Bolton, Photolysis of aqueous free chlorine species (HOCl and OCl-) with 254 nm ultraviolet light, J. Environ. Eng. Sci. 6 (2007) 277–284, https://doi.org/10.1139/S06-052.
[13] Furatian, L., 2017. The use of 185 nm radiation for drinking water treatment. University of British Columbia, Vancouver, BC. https://doi.org/10.14288/1.0348109.
[14] L. Furatian, M. Mohseni, Influence of major anions on the 185 nm advanced oxidation process - Sulphate, bicarbonate, and chloride, Chemosphere 201 (2018) 503–510, https://doi.org/10.1016/j.chemosphere.2018.02.160.
[15] M.G. Gonzalez, E. Oliveros, M. Wörner, A.M. Braun, Vacuum-ultraviolet photolysis of aqueous reaction systems, J. Photochem. Photobiol. C. Photochem. Rev. 5 (2004) 225–246, https://doi.org/10.1016/j.jphotochemrev.2004.10.002.
[16] K. Guo, Z. Wu, C. Shang, B. Yao, S. Hou, X. Yang, W. Song, J. Fang, Radical chemistry and structural relationships of PPCP degradation by UV/chlorine treatment in simulated drinking water, Environ. Sci. Technol. 51 (2017) 10431–10439.
[17] Harris, D.C., 2010. Quantitative chemical analysis. Macmillan.
[18] G.G. Jayson, B.J. Parsons, A.J. Swallow, Some simple, highly reactive, inorganic chlorine derivatives in aqueous solution. Their formation using pulses of radiation and their role in the mechanism of the Fricke dosimeter, J. Chem. Soc. Faraday Trans. 1 Phys. Chem. Condens. Phases 69 (1973) 1597–1607, https://doi.org/10.1039/F19736901597.
[19] P.D. Johnson, Mercury resonance radiation in the high-current, low-pressure discharge, JOSA 61 (1971) 1451–1454.
[20] J.A. Khan, M. Sayed, S. Khan, N.S. Shah, D.D. Dionysiou, G. Boczkaj, Advanced oxidation processes for the treatment of contaminants of emerging concern. in: Contaminants of Emerging Concern in Water and Wastewater, Elsevier, 2020, pp. 299–365.
[21] U.K. Kläning, T. Wolff, Laser Flash Photolysis of HClO, ClO−, HBrO, and BrO− in Aqueous Solution. Reactions of Cl-and Br-Atoms, Ber. der Bunsenges. F. üR. Phys. Chem. 89 (1985) 243–245, https://doi.org/10.1002/bbpc.19850890309.
[22] D.J. Lapworth, B. Lopez, V. Laabs, R. Kozel, R. Wolter, R. Ward, E.V. Amelin, T. Besien, J. Claessens, F. Delloye, Developing a groundwater watch list for substances of emerging concern: a European perspective, Environ. Res. Lett. 14 (2019) 35004.
[23] H.J. Lee, M.A. Halali, S. Sarathy, C.F. De Lannoy, The impact of monochloramines and dichloramines on reverse osmosis membranes in wastewater potable reuse process trains: A pilot-scale study, Environ. Sci. Water Res. Technol. 6 (2020) 1336–1346, https://doi.org/10.1039/d0ew00048e.
[24] Y. Lei, S. Cheng, N. Luo, X. Yang, T. An, Rate constants and mechanisms of the reactions of Cl• and Cl2•- with trace organic contaminants, Environ. Sci. Technol. (2019), https://doi.org/10.1021/acs.est.9b02462.

[25] M. Li, M. Hao, L. Yang, H. Yao, J.R. Bolton, E.R. Blatchley, Z. Qiang, Trace organic pollutant removal by VUV/UV/chlorine process: feasibility investigation for drinking water treatment on a mini-fluidic VUV/UV photoreaction system and a pilot photoreactor, Environ. Sci. Technol. 52 (2018) 7426–7433, https://doi.org/10.1021/acs.est.8b00611.
[26] M. Li, W. Li, J.R. Bolton, E.R. Blatchley III, Z. Qiang, Organic pollutant degradation in water by the vacuum-ultraviolet/ultraviolet/H2O2 process: inhibition and enhancement roles of H2O2, Environ. Sci. Technol. 53 (2018) 912–918.
[27] X.-F. Li, W.A. Mitch, Drinking water disinfection byproducts (DBPs) and human health effects: multidisciplinary challenges and opportunities, Environ. Sci. Technol. 52 (2018) 1681–1689.
[28] M. Li, Z. Qiang, P. Hou, J.R. Bolton, J. Qu, P. Li, C. Wang, VUV/UV/chlorine as an enhanced advanced oxidation process for organic pollutant removal from water: assessment with a novel mini-fluidic VUV/UV photoreaction system (MVPS), Environ. Sci. Technol. 50 (2016) 5849–5856, https://doi.org/10.1021/acs.est.6b00133.
[29] K.P. Mangalgiri, S. Patton, L. Wu, S. Xu, K.P. Ishida, H. Liu, Optimizing potable water reuse systems: chloramines or hydrogen peroxide for uv-based advanced oxidation process? Environ. Sci. Technol. 53 (2019) https://doi.org/10.1021/acs.est.9b03062.
[30] E.L. Marron, W.A. Mitch, U. Gunten, Von, D.L. Sedlak, A tale of two treatments: the multiple barrier approach to removing chemical contaminants during potable water reuse, Acc. Chem. Res. 52 (2019) 615–622, https://doi.org/10.1021/acs.accounts.8b00612.
[31] M. Masjoudi, M. Mohseni, Photolysis of chloramines in vacuum-UV and vacuum-UV/chlorine advanced oxidation processes for removal of 1, 4-dioxane: Effect of water matrix, kinetic modeling, and implications for potable reuse, J. Hazard. Mater. 454 (2023) 131454.
[32] M. Masjoudi, M. Mohseni, Photochemical properties of free chlorine and inorganic chloramines at 185 nm for VUV/UV/chlorine advanced oxidation, ACS EST Water (2022), https://doi.org/10.1021/acsestwater.1c00468.
[33] B.M. Matthew, C. Anastasio, A chemical probe technique for the determination of reactive halogen species in aqueous solution: Part 1–bromide solutions, Atmos. Chem. Phys. 6 (2006) 2423–2437, https://doi.org/10.5194/acp-6-2423-2006.
[34] R. Mertens, C. von Sonntag, Photolysis (λ= 354 nm of tetrachloroethene in aqueous solutions, J. Photochem. Photobiol. A Chem. 85 (1995) 1–9, https://doi.org/10.1016/1010-6030(94)03903-8.
[35] D.B. Miklos, C. Remy, M. Jekel, K.G. Linden, J.E. Drewes, U. Hübner, Evaluation of advanced oxidation processes for water and wastewater treatment – A critical review, Water Res 139 (2018) 118–131, https://doi.org/10.1016/j.watres.2018.03.042.
[36] Minnesota Department of Health, 2011. Carbamazepine in drinking water 2.
[37] A.S. Mora, M. Mohseni, Temperature dependence of the absorbance of 185 nm photons by water and commonly occurring solutes and its influence on the VUV advanced oxidation process, Environ. Sci. Water Res. Technol. 4 (2018) 1303–1309, https://doi.org/10.1039/C8EW00302E.
[38] S. Patton, W. Li, K.D. Couch, S.P. Mezyk, K.P. Ishida, H. Liu, Impact of the ultraviolet photolysis of monochloramine on 1, 4-dioxane removal: new insights into potable water reuse, Environ. Sci. Technol. Lett. 4 (2017) 26–30, https://doi.org/10.1021/acs.estlett.6b00444.
[39] S. Patton, M. Romano, V. Naddeo, K.P. Ishida, H. Liu, Photolysis of mono- and dichloramines in UV/hydrogen peroxide: effects on 1,4-dioxane removal and relevance in water reuse, Environ. Sci. Technol. 52 (2018) 11720–11727, https://doi.org/10.1021/acs.est.8b01023.
[40] B.S. Rathi, P.S. Kumar, P.-L. Show, A review on effective removal of emerging contaminants from aquatic systems: Current trends and scope for further research, J. Hazard. Mater. 409 (2021) 124413.
[41] A.B. Ross, B.H.J. Bielski, G.V. Buxton, D.C. Cabelli, W.P. Helman, R.E. Huie, J. Grodkowski, P. Neta, Q.G. Mulazzani, F. Wilkinson, NIST Stand. Ref. Database 40: NDRL/NIST Solut. Kinet. Database V. 3 (1998) 0.
[42] H. Schwartz, L. Marushka, H.M. Chan, M. Batal, T. Sadik, K. Fediuk, C. Tikhonov, Pharmaceuticals in source waters of 95 First Nations in Canada, Can. J. Public Heal. 112 (2021) 133–153.
[43] Z. Shu, J.R. Bolton, M. Belosevic, M.G. El Din, Photodegradation of emerging micropollutants using the medium-pressure UV/H2O2 advanced oxidation process, Water Res 47 (2013) 2881–2889.
[44] V. Sundaram, K. Pagilla, T. Guarin, L. Li, R. Marfil-Vega, Z. Bukhari, Extended field investigations of ozone-biofiltration advanced water treatment for potable reuse, Water Res 172 (2020) 115513.
[45] L. Wang, Q. Zhang, B. Chen, Y. Bu, Y. Chen, J. Ma, F.L. Rosario-Ortiz, R. Zhu, Some issues limiting photo (cata) lysis application in water pollutant control: a critical review from chemistry perspectives, Water Res 174 (2020) 115605.
[46] W. Wang, Z. Jing, Y. Zhang, Q. Wu, J. Drewes, M. Lee, U. Hubner, Assessing the chemical-free oxidation of trace organic chemicals by VUV/UV as an alternative to conventional UV/H_2O_2, Environ. Sci. Technol. 58 (16) (2024) 7113–7123, https://doi.org/10.1021/acs.est.3c08414.
[47] J.L. Weeks, G. Meaburn, S. Gordon, Absorption coefficients of liquid water and aqueous solutions in the far ultraviolet, Radiat. Res. 19 (1963) 559–567, https://doi.org/10.2307/3571475.
[48] World Health Organization(WHO). Guidance for Producing Safe Drinking-Water, 2017.
[49] World Health Organization (WHO), 1,4-Dioxane in Drinking-water. WHO Guidel, Drink. Qual. 63 (2005).
[50] Z.-Y. Xiao, N. Huang, Q. Wang, W.-L. Wang, Q.-Y. Wu, H.-Y. Hu, Advanced oxidation of dodecyl dimethyl benzyl ammonium chloride by VUV/UV/chlorine: Synergistic effect, radicals, and degradation pathway, Sep. Purif. Technol. 292 (2022) 121012, https://doi.org/10.1016/j.seppur.2022.121012.
[51] L. Yang, Z. Zhang, Degradation of six typical pesticides in water by VUV/UV/chlorine process: Evaluation of the synergistic effect, Water Res 161 (2019) 439–447, https://doi.org/10.1016/j.watres.2019.06.021.
[52] H. Zhang, W. Sun, J. Zhang, J. Ma, Vacuum-ultraviolet based advanced oxidation and reduction processes for water treatment, J. Hazard. Mater. 471 (2024) 134432, https://doi.org/10.1016/j.jhazmat.2024.134432.
[53] Y.L. Zhang, W.L. Wang, M.Y. Lee, Z.W. Yang, Q.Y. Wu, N. Huang, H.Y. Hu, Promotive effects of vacuum-UV/UV (185/254 nm) light on elimination of recalcitrant trace organic contaminants by UV-AOPs during wastewater treatment and reclamation: A review, Sci. Total Environ. 818 (2022) 151776, https://doi.org/10.1016/j.scitotenv.2021.151776.
[54] S. Zhu, B. Dong, Y. Wu, L. Bu, S. Zhou, Degradation of carbamazepine by vacuum-UV oxidation process: Kinetics modeling and energy efficiency, J. Hazard. Mater. 368 (2019) 178–185.